Aerotecnica Missili & Spazio, *The Journal of Aerospace Science, Technology and Systems*

On the Kinetic Modelling of Reactive Waves in the Hydrodynamic Limit*

Gilberto M. Kremer[a], Miriam Pandolfi Bianchi[b], Ana Jacinta Soares[c]

[a] Universidade Federal do Paraná, Brazil
Departamento de Física

[b] Politecnico di Torino, Italy
Dipartimento di Matematica

[c] Universidade do Minho, Portugal
Centro de Matemática

Abstract

The present study deals with the extension of the exact and approximate models of the Boltzmann equation to a gas mixture of four constituents undergoing a reversible bimolecular reaction, and with its application to wave propagation problems. The paper intends to highlight how such Boltzmann type models, on the basis of a shared kinetic framework, can be adopted as the starting point for a consistent derivation of the reactive hydrodynamic equations, at both the Euler and Navier Stokes limit. At this scope, a proper mathematical procedure is applied to obtain an approximate solution to the model equations, which is necessary in order to derive the closed system of the governing equations in the above said hydrodynamic limits. Resorting to this unified kinetic approach which is presented in detail, one can recognize how the dynamics of rather different wave problems well known in literature, as the steady detonation wave and its linear stability, the sound wave propagation and the light scattering phenomenon, match a satisfactory description with care for the chemical mechanism at the microscopic scale. The knowledge of the chemical process at this level permits to evaluate the influence of the chemical reaction on the fundamental aspects of the reacting gas system, reinforcing the proposed kinetic approach. Accordingly, some propagation wave problems, recently studied by the authors in this context, are in turn here reviewed at the end of focusing how their mathematical formulation and solution depend on the proposed hydrodynamic closure procedure.

1. Introduction

Physical processes where gas phase chemical reactions occur are described at various levels in literature, as documented in the books [1–3]. The investigation of chemically reacting flows is in fact fundamental in order to enlarge the knowledge of significant fields ranging from plasma chemistry to atmosphere physics at high altitudes, from ionization processes accompanying the reentry of hypersonic vehicles to chemical technology, and several others.

In particular, the kinetic study of non-equilibrium effects, and their influence on the main aspects of reactive gas systems, constitute the object of a large scientific production concerned with the chemical kinetics Boltzmann equation (BE). A chemical reaction occurring in a gas causes a perturbation of the local equilibrium, disturbing the molecular velocity distribution from its Maxwellian form and the reaction rate from its equilibrium value, whereas elastic collisions contribute to restore the equilibrium. These deviations appear to be more relevant at higher atmosphere altitudes where the elastic collisions are not sufficient to sustain the equilibrium of the gas flow, according to the interpretation given by Shizgal and Chikhaoui in Ref. [4]. A departure from the Maxwellian velocity distribution, due to the proceeding of the reaction itself, is in general responsible of the reaction rate decrease and may also induce qualitative changes of the system properties. The non-equilibrium effects arising in a dilute gas system whose constituents undergo a bimolecular chemical reaction, were recognized in the pioneering study by Prigogine and co-workers [5,6] for the simple reaction $A_1 + A_1 \rightarrow A_2 + A_3$. They first generalized the Chapman-Enskog solution of the BE to the case of reacting gases with slow chemical reactions, for which the chemical relaxation time is longer than the mechanical one. They also showed that the rate coefficient decreases from early stages of the reaction

*Based on paper presented at the XXI CEAS-AIDAA Congress, October 2011, Venice, Italy.

for which the role of products can be neglected.

The most relevant model which describes the evolution of a rarefied gas is the integro-differential BE, as widely discussed in the well known book by C. Cercignani, see Ref [7]. The integral form of the collision operator represents a mathematical complexity for both theoretical studies and numerical simulations. On the other hand, the Bhatnagar Gross and Krook (BGK)-type models, replacing the integral operator by a relaxation linear term which retains the main properties of the exact BE operator, can be more easily handled, see for example Ref. [3] and related bibliography for further details.

The present study deals with the extension of both exact BE and approximate BGK modelling to a gas mixture of four constituents undergoing a reversible bimolecular reaction.

The topics considered in this work concern the dynamics of three different wave propagation problems for a chemically reacting gas mixture, as the steady detonation wave and its linear stability, the sound wave propagation, and the light scattering phenomenon. Such problems have been modeled separately in some recent papers by the authors [8–10], and some pertinent results will be here resumed and revised according to the following aims. A first objective consists in demonstrating how it is possible to deduce a macroscopic picture in the hydrodynamic limit, starting from a kinetic description at the Boltzmann level. A further goal is to incorporate the dynamics of the above said wave problems inside a unified kinetic approach for which the starting point can be either the exact BE modelling, or the approximate BGK modelling. More in detail, the steady detonation and its linear stability are investigated when transport effects are negligible, at the Euler hydrodynamic limit of the reactive exact BE model. Conversely, the sound wave propagation and the light scattering phenomenon are studied when transport effects are relevant, at the Navier-Stokes hydrodynamic limit of the reactive approximate BGK-type model.

The paper is organized as follows. The fundamental mathematical features of the exact and approximate modellings are presented in Section 2.

The hydrodynamic closure procedure is treated in Section 3. More in detail, in Subsection 3.1, the reactive exact BE modelling is adopted to derive the reactive Euler equations in view of the steady detonation wave problem and its linear stability of Section 4. In Subsections 3.2 and 3.3 the reactive approximate BGK modelling is adopted to deduce the reactive Navier-Stokes equations and their transport properties, in view of both sound wave propagation of Section 5 and light scattering problem of Section 6.

In Section 7, final remarks and possible perspectives are presented.

2. Kinetic modelling

The main aspects of the exact BE and approximate BGK kinetic modellings, at microscopic level, are here briefly recalled in order to state the hydrodynamic picture, at the macroscopic level, which constitutes the common basis for the wave problems of Sections 4, 5 and 6.

The present modellings refer to a gas mixture of four constituents with a reversible reaction of type $A_1+A_2 \rightleftharpoons A_3+A_4$. For each constituent A_α, $\alpha = 1,2,3,4$, let m_α denote the molecular mass, with $m_1+m_2=m_3+m_4$, let ε_α be the formation energy of a molecule and $f_\alpha(t,\boldsymbol{x},\boldsymbol{c}_\alpha)$ the one-particle velocity distribution function.

At the microscopic scale, in the phase space, the evolution of the mixture is described by the kinetic equations

$$\frac{\partial f_\alpha}{\partial t} + c_i^\alpha \frac{\partial f_\alpha}{\partial x_i} = \sum_{\beta=1}^{4} \mathcal{Q}_{\alpha\beta}^E + \mathcal{Q}_\alpha^R, \tag{1}$$

where $\mathcal{Q}_{\alpha\beta}^E$ and $\mathcal{Q}_\alpha^R$ are elastic and reactive collision operators.

When the exact BE modelling is assumed, their explicit form is of integral type and it is given by

$$\mathcal{Q}_{\alpha\beta}^E = \int \left(f'_\alpha f'_\beta - f_\alpha f_\beta\right) g_{\beta\alpha}\sigma_{\beta\alpha} d\Omega_{\beta\alpha} d\mathbf{c}_\beta \tag{2}$$

$$\mathcal{Q}_1^R = \int \left[f_3 f_4 \left(\frac{m_1 m_2}{m_3 m_4}\right)^3 - f_1 f_2\right] \sigma_{12}^\star g_{21} d\Omega d\mathbf{c}_2 \tag{3}$$

where $g_{\beta\alpha} = |c_\beta - c_\alpha|$ is a relative velocity, $d\Omega_{\beta\alpha}$ and $d\Omega$ are elements of solid angles characterizing the collision processes, $\sigma_{\beta\alpha}$ is the differential elastic cross section and σ_{12}^* the reactive cross section for the forward reaction. Further reactive operators are here omitted being quite similar. For such modelling, the thermodynamical equilibrium state is assured when the constituent distribution functions f_α are the Maxwellians

$$f_\alpha^M = n_\alpha \Big(\frac{m_\alpha}{2\pi k_B T}\Big)^{\frac{3}{2}} \exp\Big(-\frac{m_\alpha (c_i^\alpha - v_i)^2}{2k_B T}\Big), \tag{4}$$

where n_α satisfy the chemical equilibrium condition given by the mass action law in the form

$$\frac{n_3 n_4}{n_1 n_2} = \Big(\frac{m_3 m_4}{m_1 m_2}\Big)^{3/2} \exp\Big(-\frac{\Delta\varepsilon}{k_B T}\Big). \tag{5}$$

Above, k_B is the Bolzmann constant, $\Delta\varepsilon = \varepsilon_3 + \varepsilon_4 - \varepsilon_1 - \varepsilon_2$ the binding energy difference, n_α the constituent number density, $\boldsymbol{v}$ the mean velocity and T the temperature of the whole mixture. When n_α are not correlated by the mass action law (5), the Maxwellians (4) define the mechanical equilibrium, only.

When the approximate BGK modelling is considered, the explicit form of elastic and reactive collision operators is homogeneous of degree one, namely

$$\mathcal{Q}^E_{\alpha\beta} = \sum_{\beta=1}^{4} \zeta^E_{\alpha\beta}(f^E_{\alpha\beta} - f_\alpha), \quad \mathcal{Q}^R_\alpha = \zeta^R_{\alpha\gamma}(f^R_{\alpha\gamma} - f_\alpha) \quad (6)$$

where $(\alpha,\gamma) = (1,2),(2,1),(3,4),(4,3)$, $\zeta^E_{\alpha\beta}$, $\zeta^R_{\alpha\gamma}$ are elastic and reactive collision frequencies. Moreover, $f^E_{\alpha\beta}$ and $f^R_{\alpha\gamma}$ are reference Gaussian distributions accounting for mixture effects and chemical effects, respectively. Further details on the collision operators are well known in literature, see for example the books [3, 7]. The considered approximate BGK collision operators have been derived in paper [9] by imposing that the production terms for mass, momentum and total energy are the same in BE and BGK models. Consequently, both modellings share the same conservation laws of mass, momentum and total energy of the mixture. In addition, the mechanical equilibrium for the approximate model is defined in terms of the Maxwellians (4), whereas the thermodynamical equilibrium is characterized by the Maxwellians (4) with the number densities n_α satisfying the mass action law (5). More specifically, the approximate model for the reactive gas flow is a relaxation model in which each constituent distribution function relaxes towards a reference Gaussian distribution, namely towards a deviation of the Maxwellian given by (4).

Another BGK modelling for a quaternary mixture with bimolecular reaction is proposed in Ref. [11], where a single BGK collision operator is considered for each α-constituent, including all elastic and reactive collisions involving the α-constituent.

The macroscopic picture, which is common to the exact modelling (2), (3) and BGK modelling (6), relevant for the wave propagation problems considered here, is provided by the hydrodynamic system

$$\frac{\partial n_\alpha}{\partial t} + \nabla\cdot(n_\alpha \boldsymbol{u}_\alpha) = \tau_\alpha, \ \alpha = 1,\dots,4, \quad (7)$$

$$\frac{\partial}{\partial t}(\varrho \boldsymbol{v}) + \nabla\cdot(\varrho \boldsymbol{v}\otimes\boldsymbol{v} + \mathbb{P}) = 0, \quad (8)$$

$$\frac{\partial}{\partial t}\Big(\frac{3}{2}nk_BT + \sum_{\alpha=1}^{4} n_\alpha\varepsilon_\alpha + \frac{1}{2}\varrho\boldsymbol{v}^2\Big) + \nabla\cdot\Big[\boldsymbol{q} + \mathbb{P}\boldsymbol{v} + \Big(\frac{3}{2}nk_BT + \sum_{\alpha=1}^{4} n_\alpha\varepsilon_\alpha + \frac{1}{2}\varrho\boldsymbol{v}^2\Big)\boldsymbol{v}\Big] = 0. \quad (9)$$

In the above system, the main independent macroscopic fields are the constituent number densities n_α, mean velocity $\boldsymbol{v}$ and temperature T of the whole mixture, with $\varrho = \sum_{\alpha=1}^{4} m_\alpha n_\alpha$ being the mixture mass density and $n = \sum_{\alpha=1}^{4} n_\alpha$ the mixture number density. Moreover τ_α and $\boldsymbol{u}_\alpha$ are the constituent reaction rate and diffusion velocity, $\mathbb{P}$ and $\boldsymbol{q}$ are the mixture pressure tensor and heat flux vector, whose kinetic definitions are

$$\tau_\alpha = \int_{\mathbb{R}^3} \mathcal{Q}^R_\alpha(f_\alpha)\, d\mathbf{c}_\alpha, \quad (10)$$

$$u^\alpha_i = \frac{1}{\varrho_\alpha}\int_{\mathbb{R}^3} m_\alpha \xi^\alpha_i f_\alpha\, d\mathbf{c}_\alpha, \quad (11)$$

$$\mathbb{P}_{ij} = \sum_{\alpha=1}^{4}\int_{\mathbb{R}^3} m_\alpha \xi^\alpha_i \xi^\alpha_j f_\alpha d\mathbf{c}_\alpha, \quad (12)$$

$$q_i = \sum_{\alpha=1}^{4}\Big(\int_{\mathbb{R}^3} \frac{1}{2} m_\alpha \xi^2_\alpha \xi^\alpha_i f_\alpha d\mathbf{c}_\alpha + n_\alpha\varepsilon_\alpha u^\alpha_i\Big), \quad (13)$$

where $\xi^\alpha = \boldsymbol{c}^\alpha - \boldsymbol{v}$ is the peculiar velocity of the α-constituent. The presence of the constitutive quantities τ_α, $\boldsymbol{u}_\alpha$, $\mathbb{P}$ and $\boldsymbol{q}$ in Eqs. (7-9) renders the hydrodynamic system non-closed, so that a closure procedure must be applied. At this end, the knowledge of f_α, which is the solution to the kinetic equations, is preliminarily required at a fixed order of approximation, as explained in the next section.

3. Hydrodynamic closures

The closure of the hydrodynamic system (7-9) is achieved once τ_α and the further fields $\boldsymbol{u}_\alpha$, $\mathbb{P}$ and $\boldsymbol{q}$ are expressed in dependence on the main macroscopic fields, through their definitions.

The Chapman-Enskog methodology is used here for a gas flow in a chemical regime close to equilibrium for which the elastic and reactive frequencies are of the same order (fast reaction regime). An approximate solution of the kinetic Eqs. (1) is determined as an expansion around the Maxwellian (4), of the form

$$\widetilde{f}_\alpha = f^M_\alpha\,[1+\phi_\alpha], \quad (14)$$

where ϕ_α represents the deviation from the mechanical equilibrium and turns out to be explicitly depending on the main macroscopic fields ϱ_α, $\boldsymbol{v}$ and T. Thus the approximation $\widetilde{f}_\alpha$ in turn depends on such main fields and is then introduced in the kinetic definitions (10-13). Such dependence is strictly related to the choice of the kinetic modelling, which can be either the exact BE or the approximate BGK equations, together with pertinent assumptions of elastic and reactive cross sections. Consequently, the structure of the elastic and reactive collision operators $\mathcal{Q}^E_{\alpha\beta}$ and $\mathcal{Q}^R_{\alpha\beta}$ is specified.

At each level of the Chapman-Enskog procedure, that is, when either $\widetilde{f}_\alpha = f^M_\alpha$ or $\widetilde{f}_\alpha = f^M_\alpha[1+\phi_\alpha]$, the constitutive laws for τ_α, $\boldsymbol{u}_\alpha$, $\mathbb{P}$ and $\boldsymbol{q}$ result from the actual computation of the integrals in definitions (10-13), once f_α is replaced by its corresponding approximation $\widetilde{f}_\alpha$.

3.1. Reactive Euler equations

At the first-order of the Chapman-Enskog method, the approximate solution $\widetilde{f}_\alpha$ is the Maxwellian f_α^M given by (4), which includes the non-equilibrium effects induced by the chemical reaction only, since the number densities n_α are not constrained by the mass action law (5). The corresponding constitutive laws are the reaction rate law

$$\tau_\alpha = \int_{\mathbb{R}^3} \mathcal{Q}_\alpha^R(f_\alpha^M)\, d\mathbf{c}_\alpha \tag{15}$$

with conditions

$$\tau_1 = \tau_2 = -\tau_3 = -\tau_4, \tag{16}$$

which assure the correct chemical exchanges predicted by the reaction, and the further laws for $\boldsymbol{u}_\alpha$, $\mathbb{P}$ and $\boldsymbol{q}$

$$\boldsymbol{u}_\alpha = 0, \quad \mathbb{P} = pI, \quad \boldsymbol{q} = 0, \tag{17}$$

where I represents the identity matrix and p the mixture pressure, with $p = nk_BT$.

The hydrodynamic system closed at this level consists in Eqs. (7-9) together with the constitutive laws (15-17). The resulting system defines the reactive Euler equations which are appropriate when the transport effects are absent. Such system is the mathematical tool for the kinetic description of the steady detonation wave and its linear stability in Section 4.

3.2. Reactive Navier-Stokes equations

At the second-order of the expansion procedure, the approximate solution $\widetilde{f}_\alpha$ in the form (14) is characterized in terms of the deviation ϕ_α containing the effects of the transport fluxes. The corresponding constitutive laws are then the reaction rate law

$$\tau_\alpha = \int_{\mathbb{R}^3} \mathcal{Q}_\alpha^R(f_\alpha^M\,[1+\phi_\alpha])\, d\mathbf{c}_\alpha \tag{18}$$

and the generalized Fick, Navier-Stokes and Fourier laws, which are respectively given by

$$u_i^\alpha = \frac{1}{\varrho_\alpha}\int_{\mathbb{R}^3} m_\alpha \xi_i^\alpha f_\alpha^M \phi_\alpha\, d\mathbf{c}_\alpha, \tag{19}$$

$$\mathbb{P}_{ij} = p\,\delta_{ij} + \sum_{\alpha=1}^{4}\int_{\mathbb{R}^3} m_\alpha \xi_i^\alpha \xi_j^\alpha f_\alpha^M \phi_\alpha d\mathbf{c}_\alpha, \tag{20}$$

$$q_i = \sum_{\alpha=1}^{4}\Bigg(\int_{\mathbb{R}^3}\frac{1}{2} m_\alpha \xi_\alpha^2 \xi_i^\alpha f_\alpha^M \phi_\alpha d\mathbf{c}_\alpha + \varepsilon_\alpha \int_{\mathbb{R}^3} \xi_i^\alpha f_\alpha^M [1+\phi_\alpha] d\mathbf{c}_\alpha\Bigg). \tag{21}$$

The hydrodynamic system closed at this level consists then in Eqs. (7-9) together with the constitutive laws (18-21). The resulting system defines the reactive Navier-Stokes equations, which is appropriate when the transport effects are taken into account. Note that Eq. (20) expresses the constitutive law of a Newtonian fluid which, in kinetic theory, is also called the Navier-Stokes law [7, 12]. When the kinetic modelling of the collisional dynamics is chosen on the basis of the selected collision operators, the deviation ϕ_α can be explicitly determined and the constitutive laws (19-21) permit to detail the transport picture through the actual computation of the transport coefficients.

3.3. Transport properties

The transport picture is here represented starting from the kinetic modelling of Section 2 adopting the BGK collision operators, hard-spheres elastic cross sections and Present's reactive cross sections. Therefore, the generalized Fick, Navier-Stokes and Fourier laws are deduced from the constitutive Eqs. (18-21) in the form

$$d_i^\alpha = -\sum_{\beta=1}^{4}\frac{x_\alpha^{\rm eq} x_\beta^{\rm eq}}{D_{\alpha\beta}}\left(u_i^\alpha - u_i^\beta\right), \tag{22}$$

$$\mathbb{P}_{ij} = p\delta_{ij} - \mu\left(\frac{\partial v_i}{\partial x_j} + \frac{\partial v_j}{\partial x_i} - \frac{2}{3}\frac{\partial v_r}{\partial x_r}\delta_{ij}\right), \tag{23}$$

$$q_i = -\lambda\frac{\partial T}{\partial x_i} + \sum_{\alpha=1}^{4}\left(\frac{5}{2}k_BT + \varepsilon_\alpha\right) n_\alpha^{\rm eq} u_i^\alpha, \tag{24}$$

where $x_\alpha^{\rm eq} = n_\alpha^{\rm eq}/n^{\rm eq}$ denote equilibrium molar fractions, d_i^α the constituent diffusion forces and $D_{\alpha\beta}$, μ and λ are the diffusion, shear viscosity and thermal conductivity coefficients. They turn out to be known functions of T, n_α and both elastic and reactive collision frequencies $\zeta_{\alpha\gamma}^E$ and $\zeta_{\alpha\gamma}^R$, through the expressions

$$\frac{1}{D_{\alpha\gamma}} = \frac{1}{D_{\gamma\alpha}} = \frac{m_{\alpha\gamma}}{k_BTx_\gamma^{\rm eq}}\left[\zeta_{\alpha\gamma}^E + \frac{2}{3}\zeta_{\alpha\gamma}^R\left(\epsilon_\sigma^\star + \frac{1}{2}\right)\right], \tag{25}$$

$$\frac{1}{D_{\alpha\delta}} = \frac{1}{D_{\delta\alpha}} = \frac{m_{\alpha\delta}}{k_BTx_\delta^{\rm eq}}\left[\zeta_{\alpha\delta}^E + \zeta_{\alpha\gamma}^R\frac{m_\alpha + m_\delta}{m_\alpha + m_\gamma}\right], \tag{26}$$

$$\mu = \sum_{\alpha=1}^{4}\frac{n_\alpha^{\rm eq}k_BT}{\zeta_{\alpha\gamma}^R + \sum_{\beta=1}^{4}\zeta_{\alpha\beta}^E}, \tag{27}$$

$$\lambda = \frac{5}{2}\sum_{\alpha=1}^{4}\frac{n_\alpha^{\rm eq}k_B^2T/m_\alpha}{\zeta_{\alpha\gamma}^R + \sum_{\beta=1}^{4}\zeta_{\alpha\beta}^E}, \tag{28}$$

where (α,γ) are defined as in Eq.(6), $\delta \neq \gamma$ for each fixed α, and $\epsilon_\sigma^\star = \epsilon_\sigma/k_BT$ is the activation energy in units of k_BT. Moreover, σ takes the values 1 and -1 for the reactants ($\alpha = 1, 2$) and products ($\alpha = 3, 4$) of the reaction, $\epsilon_1^\star$ denotes the forward activation energy, whereas $\epsilon_{-1}^\star$ the backward activation energy.

The behaviour of the transport coefficients for the elementary reaction $H_2 + Cl \rightleftharpoons HCl + H$ of the Hydrogen-Chlorine system is investigated for one mole only of an ideal gas mixture, for which the total number density is $n = 2.6 \times 10^{25}$ molecules/m^3 and the equilibrium

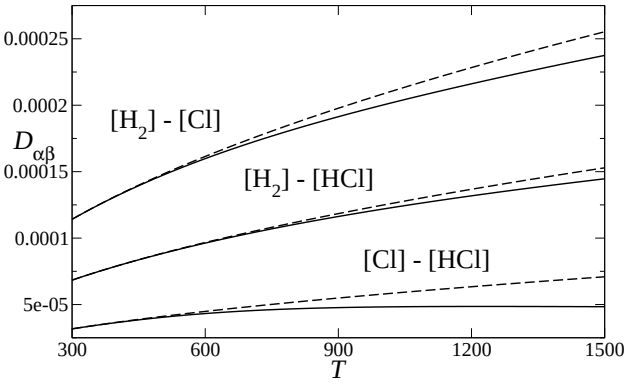

Figure 1. Diffusion coefficients $D_{\alpha\beta}$ (m^2/s) as function of T (K). Dashed line: inert mixture; solid line: reactive mixture.

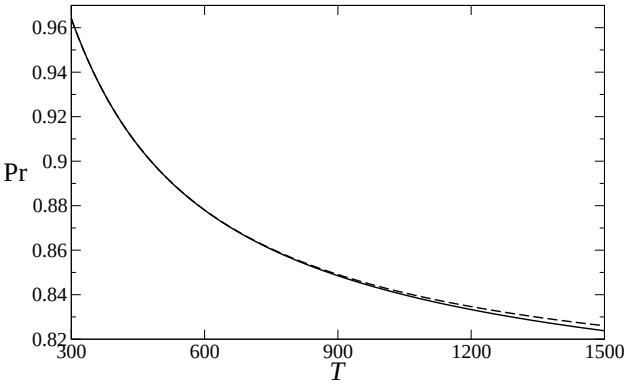

Figure 2. Prandtl number as function of T (K). Dashed line: inert mixture; solid line: reactive mixture.

molar fractions are such that $x_1^{\rm eq} = x_2^{\rm eq}$ and $x_3^{\rm eq} = x_4^{\rm eq}$. The influence of the chemical reaction on the transport picture is appreciated comparing the results for the reactive mixture with those obtained in absence of chemical reaction. Figure 1 shows the behaviour of three diffusion coefficients $D_{\alpha\beta}$ in dependence on the mixture temperature T for the reactive mixture (solid line) and for the inert one (dashed line). The picture illustrates an increasing behaviour with T which is more pronounced for the inert mixture. The behaviour of the other diffusion coefficients, as well as that of viscosity and thermal conductivity, is quite similar and, for brevity, is not reported here.

Moreover the Prandtl number of the considered mixture, whose kinetic definition is given by

$$\Pr = \frac{5\mu}{2\lambda}\left[\frac{4k_B(n_1^{\rm eq}+n_2^{\rm eq}+n_3^{\rm eq}+n_4^{\rm eq})}{m_1 n_1^{\rm eq}+m_2 n_2^{\rm eq}+m_3 n_3^{\rm eq}+m_4 n_4^{\rm eq}}\right], \quad (29)$$

is represented in Fig. 2. The results show a decreasing behaviour of Pr with T, as expected, and an acceptable range of values of Pr, lying inside the difference between the BGK approximation and the exact BE evaluation for the Prandtl number of a single gas.

4. Steady detonation waves: propagation and stability

In this section the kinetic modelling of Section 2 with hydrodynamic closure at the Euler level, as specified in Subsection 3.1, is applied to study the dynamics of a planar detonation wave and its linear stability. The wave propagates in an explosive gas mixture, in a flow regime for which mechanical equilibrium and strong chemical disequilibrium hold, and diffusion, shear viscosity and heat flux are absent. The formulation of the detonation problem is founded on to the well-known Zeldovich, Von Neumann and Doering (ZND) model, see Ref. [13], specialized to one space dimension. The structure of the planar steady detonation wave is represented in Fig. 3. A non-reactive shock wave propagates with constant velocity D in a quiescient gas mixture. Such wave is sustained by the energy release of an exothermic chemical reaction which occurs in the reaction zone attached to the shock. At last, the following flow can be either a constant flow (overdriven detonation) or a rarefaction followed by a constant flow (unsupported detonation). The initial state, ahead of the shock, is denoted by I and represents the unreacted gas mixture. The von Neumann state N, just ahead of the shock, represents the still unreacted mixture with very hight pressure. Behind the shock front, the intermediates states of partial chemical reaction, are represented by R, whereas the final state of chemical equilibrium is denoted by S. The kinetic modelling is based on the exact BE collision operators, and on a particular choice of reactive cross sections with threshold energy, which satisfy the micro-reversibility principle and extends the Present model, see Ref. [3].

Therefore, the hydrodynamic system is obtained reducing to one space dimension Eqs. (7-9), constitutive laws (17) and rate law (15) expressed in the form

$$\tau_\alpha = \left[-n_1 n_2\left(\frac{m_3 m_4}{m_1 m_2}\right)^{3/2}\exp\left(-\frac{\Delta\varepsilon}{k_B T}\right)+n_3 n_4\right]S_\alpha, \quad (30)$$

where S_α is a suitable weight function depending on temperature and threshold velocity, whose expression is specified in Ref. [14].

The governing equations of the explosive mixture directly follow from the one-dimensional reactive Euler

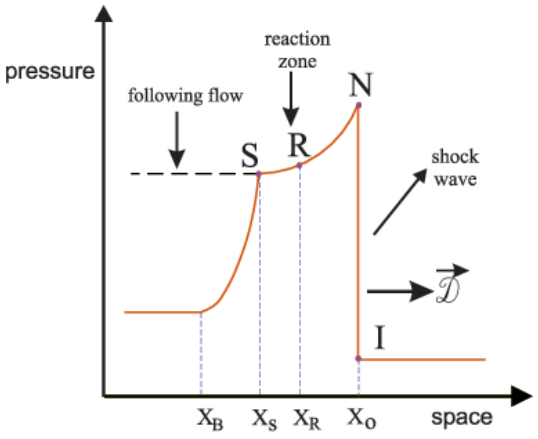

Figure 3. ZND structure of the detonation wave.

equations, referred to the steady frame attached to the shock. Thus the governing equations assume the form

$$(v-\mathcal{D})\frac{dn_1}{dx}+n_1\frac{dv}{dx}=\tau_1, \tag{31}$$

$$(v-\mathcal{D})\frac{d}{dx}(n_1+n_3)+(n_1+n_3)\frac{dv}{dx}=0, \tag{32}$$

$$(v-\mathcal{D})\frac{d}{dx}(n_1+n_4)+(n_1+n_4)\frac{dv}{dx}=0, \tag{33}$$

$$(v-\mathcal{D})\frac{d}{dx}(n_2+n_3)+(n_2+n_3)\frac{dv}{dx}=0, \tag{34}$$

$$(v-\mathcal{D})\frac{dv}{dx}+\frac{1}{\varrho}\frac{dp}{dx}=0, \tag{35}$$

$$(v-\mathcal{D})\frac{d}{dx}\Big(\frac{3}{2}nk_BT+\sum_{\alpha=1}^{4}n_\alpha\varepsilon_\alpha+\frac{1}{2}\varrho v^2\Big) \tag{36}$$

$$+\Big(\frac{3}{2}nk_BT+\sum_{\alpha=1}^{4}n_\alpha\varepsilon_\alpha+\frac{1}{2}\varrho v^2\Big)\frac{dv}{dx}+\frac{d(pv)}{dx}=0.$$

The rate equation (31) defines the progress of the chemical reaction, since it describes the space evolution of the number density of the constituent A_1. Moreover Eqs. (32-36) represent the conservation laws of partial number densities, as well as momentum and total energy of the whole mixture. The integration of these equations between the initial state, ahead of the shock, and any state in the reaction zone, namely the von Neumann N, the intermediate state R and the final state S, leads to the Rankine-Hugoniot (RH) conditions which, as known, connect the fluxes of the main fields between the initial quiescent mixture and the explosive mixture in the reaction zone.

The system formed by the rate equation (31) together with the algebraic RH conditions must be solved with suitable initial conditions and input parameters in order to characterize the main fields n_α, v, T at the von Neuman, intermediate and final states, for an overdriven detonation. The knowledge of such fields specifies the structure of the detonation wave, including the wave thickness corresponding to the spatial distance between the von Neuman and final states. Numerical simulations have been performed, according to Ref. [15], for an elementary reaction of the explosive hydrogen-oxygen chain, $H_2O+H \rightleftharpoons OH+H_2$. In particular, the behaviour of the mixture number density n is represented in Fig. 4 versus the wave thickness. The input data for the initial state are represented in Table 1, and the values for binding energy difference, detonation wave velocity and Mach number are

$$\Delta\varepsilon = 63311\,\mathrm{Jmol}^{-1},\ D=3500\,\mathrm{ms}^{-1},\ M=1.6888.$$

Table 1
Constituent number densities n_α ($\mathrm{mol\,l}^{-1}$), number density n ($\mathrm{mol\,l}^{-1}$), temperature T (K), and mean velocity v (ms^{-1}) of the mixture, evaluated at the Von Neumann state (N) and final state (S), for given initial state (I).

	State S	State N	State I
n_1	0.30112	0.10590	0.03000
n_2	0.27563	0.07060	0.02000
n_3	0.03014	0.35300	0.10000
n_4	0.28496	0.70601	0.20000
n	0.89185	1.23551	0.35000
T	2363.16	2357.89	298.15
v	2126.46	2508.51	0

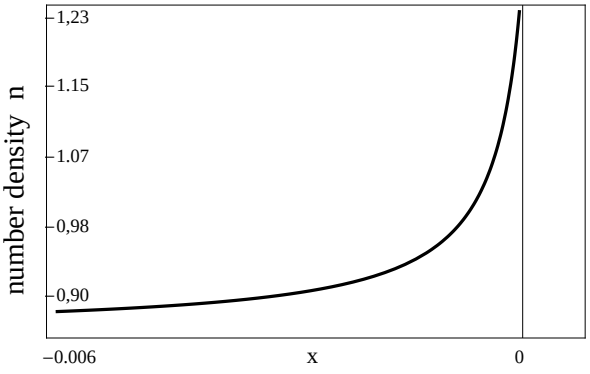

Figure 4. Detonation wave profile of number density n versus the wave thickness, for Mach number $M=1.6888$ and detonation velocity $\mathcal{D}=3500ms^{-1}$.

The linear stability of the steady detonation wave constitutes a relevant problem, classically treated in a wide literature of the last decades. The reader can be addressed, for instance, to Ref. [16] and related bibliography. This problem can also be investigated

starting from the mathematical modelling presented in its general form in Sections 2 and 3.

The stability is studied analysing the response of the steady solution to small rear boundary perturbations which induce a distortion $\psi(t)$ in the position of the planar shock wave. Consequently, such distortion affects the steady wave solution and results in the perturbation of the main fields in the reaction zone. The knowledge of the evolution of the main field perturbations is the goal for the solution to the stability problem. The decay in time of all field perturbations corresponds to a stable behaviour; conversely, a growth in time of at least one field perturbation implies an unstable solution.

The stability problem, referred to the detonation wave solution characterized in this section, first requires the linearization of the one dimensional reactive Euler equations and RH conditions. Normal mode expansions with exponential time dependent perturbations, around the steady detonation solution, are considered for the main fields, in the form

$$\begin{aligned} \boldsymbol{z}(x,t) &= \boldsymbol{z}^*(x) + \exp(at)\,\overline{\boldsymbol{z}}(x), \\ \psi(t) &= \overline{\psi}\exp(at), \quad a, \overline{\psi} \in \mathbb{C}, \quad a = \alpha + i\beta. \end{aligned} \tag{37}$$

Above, $\boldsymbol{z}(x,t)$ represents the vector of the perturbed main fields, $\boldsymbol{z}^*(x)$ the steady detonation solution, $\overline{\boldsymbol{z}}(x)$ the unknown space disturbances, $\overline{\psi}$ the complex amplitude of the shock distortion, α and β the perturbation growth rate and frequency. Inserting the above expansions (37) into the one dimensional reactive Euler equations, the stability equations turn out as a system of linear ODE's formulated in terms of the eigenfunctions $\overline{\boldsymbol{z}}(x)$ and eigenvalues $a = \alpha + i\beta$. Consequently, the sign of the real part of the eigenvalue, say α, determines the stability behaviour of the steady solution.

The RH conditions, linearized as well, provide the initial conditions for the stability problem. Since this system involves the unknown eigenvalue a, a further equation is required to assure the determinacy of the stability problem. This closure condition has been derived in paper [17] and results to be the dispersion relation of the normal modes. It expresses the physical meaning that the reaction zone is acoustically isolated from the rear boundary.

The system formed by the stability equations, together with the RH conditions and dispersion relation, furnishes the stability solution, namely the space disturbances of the main fields, the growth rate α and time frequency β of the oscillations.

Numerical simulations are performed in agreement with the results of paper [8], for the explosive hydrogen-oxygen mixture. The influence of the disturbances $\exp(at)\,\overline{\boldsymbol{z}}(x)$ on the steady solution $\boldsymbol{z}^*(x)$ can be evaluated by means of the behaviour of $\mathrm{Re}[\exp(at)\,\overline{\boldsymbol{z}}(x)]$. In particular such influence on the mass density ϱ^* of the mixture, say $\overline{\varrho}$ for simplicity, is

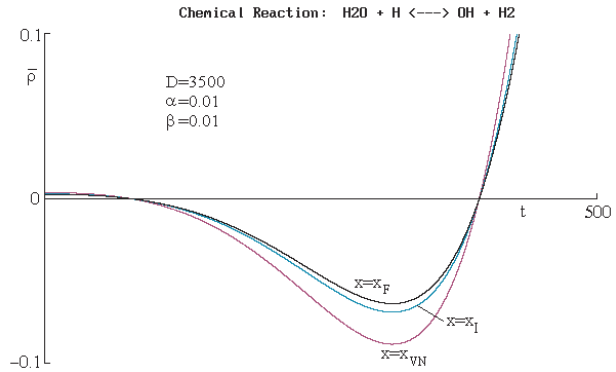

Figure 5. Instability behaviour of the mass density perturbation versus time at different states, for growth rate $\alpha = 0.01$ and disturbance frequency $\beta = 0.01$.

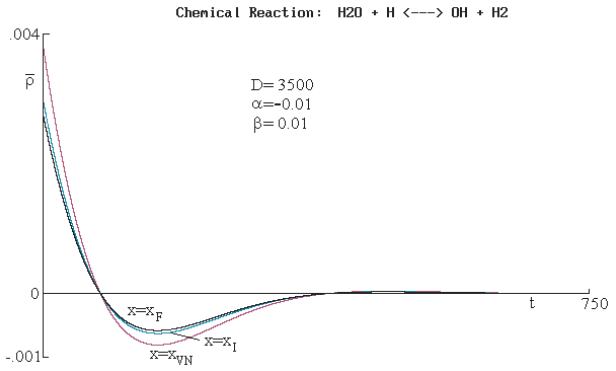

Figure 6. Stability behaviour of the mass density perturbation versus time at different states, for growth rate $\alpha = -0.01$ and disturbance frequency $\beta = 0.01$.

represented by

$$\overline{\varrho} = \sum_{i=1}^{4} e^{\alpha t}\Big(\cos\beta t\,\mathrm{Re}\overline{z}_i(x) - \sin\beta t\,\mathrm{Im}\overline{z}_i(x)\Big).$$

Figure 5 shows the time behaviour of $\overline{\varrho}$ for a positive value of the growth rate, that is for $\alpha = 0.01$, and frequency $\beta = 0.01$. The picture indicates a typical instability behaviour of the steady solution. The curves are drawn for the von Neuman ($x = x_{VN}$), intermediate ($x = x_I$), and final state ($x = x_F$), respectively. Analogously, Fig. 6 shows the time behaviour of $\overline{\varrho}$ for $\alpha = -0.01$, and thus indicates a typical stability behaviour of the steady solution.

5. Sound wave propagation

In this section, the propagation of sound waves in a reactive mixture where the transport effects are relevant is studied at the Navier-Stokes, Fourier and Fick level, according to Subsections 3.2 and 3.3. The kinetic modelling is based on the approximate BGK collision operators, and Present's reactive cross sections. The hydrodynamic system is formed by Eqs. (7-9) reduced to one space dimension and closed with the constitutive laws (22-24) and rate law in the form

$$\tau_\alpha = \nu_\alpha n_\alpha n_\gamma k_\sigma^{(0)} \frac{\mathcal{A}}{k_B T}, \tag{38}$$

where $k_\sigma^{(0)}$ is the first approximation to the forward ($\sigma = 1$) and backward ($\sigma = -1$) rate constants, $\mathcal{A}$ is the affinity of the forward chemical reaction, and $\gamma = 2, 1, 4, 3$ for $\alpha = 1, 2, 3, 4$, respectively.

The kinetic dynamics of longitudinal sound waves is studied assuming that planar harmonic waves of small amplitude propagate along the x-direction in the reactive mixture at equilibrium state characterized by $n_\alpha^{(\mathrm{eq})}$, T_0 and vanishing velocity. The closed system of hydrodynamic equations is then linearized around the equilibrium state assuming harmonic sound wave expansions of the form

$$\begin{aligned} \widetilde{n}_\alpha &= n_\alpha^{(\mathrm{eq})} + \overline{n}_\alpha \exp[\imath(\kappa x - \omega t)], \\ \widetilde{v} &= \overline{v} \exp[\imath(\kappa x - \omega t)], \\ \widetilde{T} &= T_0 + \overline{T} \exp[\imath(\kappa x - \omega t)]. \end{aligned} \tag{39}$$

Above, $\overline{n}_\alpha$, $\overline{v}$, $\overline{T}$ represent complex amplitudes of the sound waves, and κ, ω are the complex wave number and real angular frequency, respectively. The linearization through expansions (39) leads to the dispersion relation of the wave solutions, which can be solved in order to express the wave frequency κ in dependence on ω. The dispersion and the attenuation of the sound waves are represented through the wave phase velocity $v_{ph} = \omega/\mathrm{Re}\,\kappa$ and the attenuation coefficient $\alpha = \mathrm{Im}\,\kappa$. Numerical simulations are performed for two mixtures of the Hydrogen-Chlorine system, where the elementary reaction $\mathrm{H_2{+}Cl} \rightleftharpoons \mathrm{HCl{+}H}$ takes place. The first, case (a), with equilibrium molar fractions $x_1^{\mathrm{eq}} = 0.1$, $x_2^{\mathrm{eq}} = 0.618$, $x_3^{\mathrm{eq}} = 0.082$, $x_4^{\mathrm{eq}} = 0.2$, and the second, case (b), with $x_1^{\mathrm{eq}} = 0.2$, $x_2^{\mathrm{eq}} = 0.424$, $x_3^{\mathrm{eq}} = 0.076$, $x_4^{\mathrm{eq}} = 0.3$. The simulations have been performed for $T_0 = 1500\mathrm{K}$ and $\Delta\varepsilon = 3.98\,\mathrm{kJmol}^{-1}$.

Figures 7 and 8 illustrate the trend of v_0/v_{ph} and $\alpha v_0/\omega$ versus ω (GHz), for the so called first sound wave propagating in the positive x-direction. In particular, v_0 is the computed sound velocity of the corresponding non reactive Eulerian mixture. More in detail, both pictures refer to the first mixture, case (a), in presence of the chemical reaction (dot line) and in its absence (solid line), as well as to the second mixture, case (b), in presence of the chemical reaction (dot-dashed line) and in its absence (dashed line).

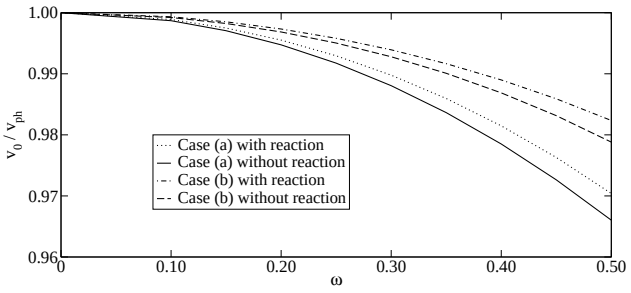

Figure 7. Phase velocity for two mixtures of the H_2-Cl system, cases (a) and (b), versus the angular frequency ω (GHz).

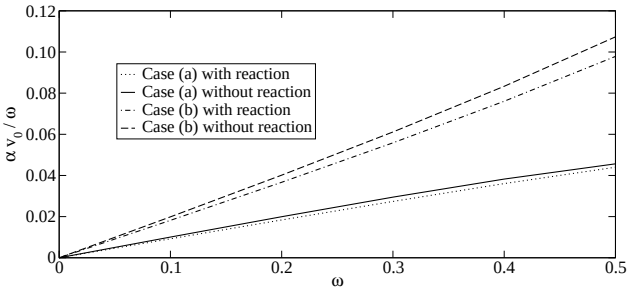

Figure 8. Attenuation coefficient for two mixtures of the H_2-Cl system, cases (a) and (b), versus the angular frequency ω (GHz).

These figures evidence that the phase velocity and attenuation coefficient are smaller for the reactive mixtures than for the corresponding inert ones and that the influence of the chemical reaction becomes negligible at lower frequencies. This behaviour is consistent with the results of Subsection 3.3 on the transport properties and is justified by the fact that the transport coefficients are smaller for reactive mixtures than for the corresponding inert ones. Moreover the results are in agreement with those obtained in paper [9] for the same reactive system but with different concentrations.

6. Light scattering spectra

In this section, the wave propagation of the light scattered by a reactive mixture where the transport effects are relevant, is studied starting from the hydrodynamic closure at the Navier-Stokes, Fourier and

Fick level, derived in Subsections 3.2 and 3.3. This study aims to describe the response of the reactive mixture in thermodynamical equilibrium to the incident light field. More specifically, the incident light induces small deviations on the basic fields from the equilibrium values, according to the expansions

$$n_\alpha = n_\alpha^{\rm eq} + \widetilde{n}_\alpha, \quad v_i = \widetilde{v}_i, \quad T = T_0 + \widetilde{T}, \qquad (40)$$

around constant number densities and mixture temperature of an equilibrium state with vanishing mean velocity. The evolution of such deviations obeys to the linearized equations, derived from the hydrodynamic system closed at the Navier-Stokes, Fourier and Fick level. The role of these deviations, and in particular that of the constituent number densities, will result evident in the sequel. In this paper, the kinetic approach to the light scattering problem is considered in the spirit of the previous applications of Section 4 and Section 5, and can be made more comprehensible if some brief preliminaries are provided, with reference to the book [18] by Berne and Pecora.

When a monochromatic linearly polarized plane light wave impinges upon a gas mixture, the interaction of the light field with the gas determines the deviations of the light itself, caused by the dielectric constant fluctuations. It is possible to evaluate the intensity of the light scattered by the mixture in terms of the constituent number density perturbations $\widetilde{n}_\alpha$, introduced in expansions (40.)

The mathematical tool to be used for the description of the light scattering spectra is the so called dynamic structure factor $S(\mathbf{q},\omega)$, $\mathbf{q}$ being the change in the wave vector and ω the shift in the angular frequency of the scattered light. This factor is classically defined in terms of the auto correlation of the Laplace-Fourier transform of the dielectric constant fluctuations, namely

$$S(\mathbf{q},\omega) = {\rm Re}\big[\langle \delta\epsilon(\mathbf{q},i\omega)\delta\epsilon(\mathbf{q},0)\rangle\big]. \qquad (41)$$

It is possible now to express $S(\mathbf{q},\omega)$ in dependence on the constituent number density perturbations $\widetilde{n}_\alpha(\mathbf{q},i\omega)$, in place of the dielectric constant fluctuations $\delta\epsilon(\mathbf{q},i\omega)$, first resorting to the Clausius-Mossotti equation, see Ref. [19], and then invoking the Onsager reciprocity regression hypothesis, see Ref. [20]. Thus, the final expression of $S(\mathbf{q},\omega)$ results to be

$$S(\mathbf{q},\omega) = \sum_{\alpha,\gamma=1}^{4} a_\alpha a_\gamma {\rm Re}\left[\langle \widetilde{n}_\alpha(\mathbf{q},i\omega)\,\widetilde{n}_\gamma(\mathbf{q},0)\rangle\right]. \qquad (42)$$

where a_α denotes the constituent polarizability. The presence of $\widetilde{n}_\alpha(\mathbf{q},i\omega)$ in Eq. (42) indicates that $S(\mathbf{q},\omega)$ can be characterized in the kinetic frame, starting from the hydrodynamic Eqs. (7-9) closed with the constitutive laws (22-24) and rate law (38). More specifically, the hydrodynamic system and the closure conditions must be first linearized according to expansions (40) and successively Laplace-Fourier transformed.

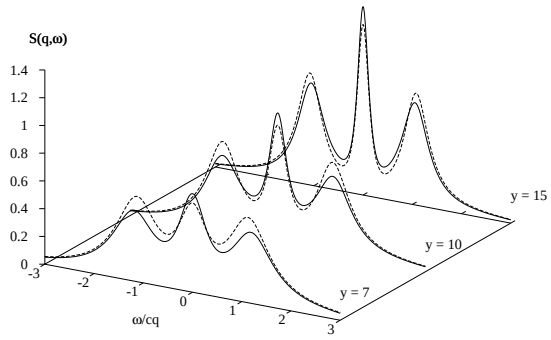

Figure 9. Case (a). Dynamic structure factor versus the reduced angular frequency, for different values of the uniformity parameter y. Reactive mixture (solid line) and inert mixture (dashed line).

Some numerical simulations in order to evaluate the dynamic structure factor are performed in agreement to Ref. [10], for two different mixtures of the Hydrogen-Chlorine system, where the chemical reaction H_2+Cl $\rightleftharpoons$ HCl+H occurs. Also in this application the influence of the chemical reaction can be evaluated. Thus the behaviour of $S(\mathbf{q},\omega)$ referred to the reactive mixture is compared with the behaviour of $S(\mathbf{q},\omega)$ referred to the corresponding inert mixture.

The light scattering spectrum, evidencing the Rayleigh and Brillouin peaks, is represented in Figs. 9 and 10 as function of the reduced angular frequency $\omega/(cq)$, for different values of the uniformity parameter y. This parameter is defined as $y = 1/(q\tau c)$, that is the ratio between the wavelength $1/q$ of the incident light and the effective mean free path τc, τ being an effective relaxation time, and c the adiabatic sound speed. The range of y assures that the hydrodynamic equations can be used to describe $S(q,\omega)$ for the given mixture.

Two mixtures are analyzed with different equilibrium constituent concentrations and same equilibrium temperature $T_0 = 1500$K, namely *case* (a) $x_1^{\rm eq} = x_2^{\rm eq} = 0.33$, $x_3^{\rm eq} = x_4^{\rm eq} = 0.17$ and *case* (b) $x_1^{\rm eq} = 0.1$, $x_2^{\rm eq} = 0.618$, $x_3^{\rm eq} = 0.082$, $x_4^{\rm eq} = 0.2$. The simulations are performed for $y = 7$, $y = 10$ and $y = 15$.

In both cases, for increasing y, the intensity of the peaks grows and they become narrower. As known in literature, see for example book [18], the typical Rayleigh and Brillouin triplet consists of a central Rayleigh peak and two side Brillouin peaks symmetrically shifted around the origin. They are are perfectly evident in Figs. 9 and 10. On the other hand, the Rayleigh and Brillouin peaks are less sharp in case (b) than in case (a). This is due to the fact that the partial

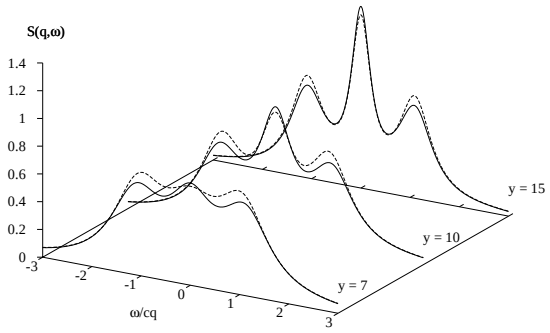

Figure 10. Case (b). Dynamic structure factor versus the reduced angular frequency, for different values of the uniformity parameter y. Reactive mixture (solid line) and inert mixture (dashed line).

uniformity parameters and the partial polarizabilities must be considered.

7. Conclusions

In this paper, the common features of the kinetic approach, based on either the exact or the approximate extended models of the Boltzmann equation, are highlighted and reworked to formulate and solve different wave problems for reactive gas mixtures. The steady detonation wave and its linear stability, the sound wave propagation and the light scattering, which have been previously treated by the authors in Refs. [8], [9] and [10], are here revisited as pertinent fluidynamical applications of the proposed kinetic methodology.

In view of a unified macroscopic description in the hydrodynamic limit for the considered reactive flow, and in particular for the dynamics of its wave propagation in the various cases, the paper shows that the analytical closure of the nonlinear system of the field hydrodynamic equations always plays a shared central role. The expected final results of each application confirm an appreciable agreement with the ones known in classical literature. Furthermore, the last application in the present paper, namely the light scattering problem, even though it could seem to be far away from the previous wave propagation problems, in particular due to its rather strong physical and mathematical complexity, is presented and investigated in such a way that its dependence on the kinetic closure procedure appears to be completely justified.

The following improvements and extensions, however, can be considered.

The study of the steady detonation wave and its linear stability could include the heat of reaction and the dissipative contribution due to an endothermic reaction, as well as the transport effects. In addition, this analysis could be extended to the bi-dimensional case.

The dynamics of acoustic waves and light scattering could be investigated starting from the exact BE rather than resorting to the approximate BGK equation in order to include further transport effects in wave propagation. Thus, a more detailed description of the transport picture, which would include thermal diffusion and diffusion-thermal effects, may also be developed, in spite of the much more complicate computations.

Acknowledgments

The paper is partially supported by Brazilian Research Council (CNPq), by Italian National Project GNFM 2010/11 and by Minho University Mathematics Centre (CMAT), FEDER–COMPETE Funds, FCT–Project Est-C/MAT/UI0013/2011.

REFERENCES

1. R. Brun, "Introduction to Reactive Gas Dynamics", *Oxford University Press*, NewYork, 2009.
2. E. Nagnibeda and E. Kustova, "Non-Equilibrium Reacting Gas Flows: Kinetic Theory of Transport and Relaxation Processes", *Springer Verlag*, Berlin, 2009.
3. G. M. Kremer, "An introduction to the Boltzmann equation and transport processes in gases", *Springer*, Berlin, 2010.
4. B. D. Shizgal and A. Chikhaoui, "On the use temperature parameterized rate coefficients in the estimation of non-equilibrium reaction rates", *Physica A*, Vol. 365, pp. 317–332, 2006.
5. I. Prigogine and E. Xhrouet, "On the perturbation of maxwell distribution function by chemical reactions in gases", *Physica*, Vol. 15, pp. 913–932, 1949.
6. I. Prigogine and M. Mahieu, "Sur la perturbation de la distribution de Maxwell par des réactions chimiques en phase gazeuse", *Physica*, Vol. 16, pp. 51–64, 1950.
7. C. Cercignani, "Theory and application of the Boltzmann equation", *Scottish Academic Press*, Edinburgh, 1975.
8. M. Pandolfi Bianchi and A. J. Soares, "Modelling and solutions to the linear stability of a detonation wave in the kinetic frame", *J. Difference Eqs. App.*, Vol. 17, pp. 1169–1184, 2011.
9. G. M. Kremer, M. Pandolfi Bianchi and A. J. Soares, "A relaxation kinetic model for transport phenomena in a reactive flow", *Phys. Fluids*, Vol. 18, 037104, pp. 1–15, 2006.
10. G. M. Kremer, W. Marques Jr., M. Pandolfi Bianchi and A. J. Soares, "Spectral Distribution of Scattered Light from a Chemical Relaxation System", *Rarefied Gas Dynamics*, AIP Proceedings, Eds. D. A. Levin, I. J. Wysong and A. L. Garcia, Vol. 1333, 2011, pp. 673–678.
11. M. Groppi and G. Spiga, "A Bhatnagar-Gross-Krook-type approach for chemically reacting gas mixtures", *Phys.Fluids*, Vol. 16, pp. 4273–4284, 2009.
12. M. Bisi, M. Groppi, G. Spiga, "A Kinetic Model for Bimolecular Chemical Reactions", in *Kinetic Methods for Nonconservative and Reacting Systems*, *Aracne Editrice*, Naples, 2005.
13. W. Fickett, "Introduction to Detonation Theory", *University of California*, Berkeley, 1986.
14. P. Griehsnig, F. Schürrer and G. Kügerl, "Kinetic theory for particles with internal degrees of freedom", *Rarefied Gas Dynamics: Theory and Simulations*, AIAA, Washington, Vol. 159, pp. 581–589, 1992.
15. R. Monaco, M. Pandolfi Bianchi and A. J. Soares, "A Ki-

netic Approach to Propagation and Stability of Detonation Waves", *Rarefied Gas Dynamics*, AIP Proceedings, Ed. Abe T., Vol. 1084, pp. 45–50, 2009.
16. D. S. Stewart and A. Kasimov "State of Detonation Stability Theory and Its Application to Propulsion", *J. Propul. Power*, **22**, 1230-1244 (2006).
17. A. Kasimov and D. S. Stewart, "Spinning instability of gaseous detonations", *J. Fluid Mech.*, **466**, 179-203 (2002).
18. B. Berne and R. Pecora, "Dynamic Light Scattering", *Wiley*, New York, 1976.
19. M. Born, E. Wolf, *Principles of Optics*, Cambridge University Press, Cambridge, 1999.
20. W. Weiss, I. Muller, Continuum Mech. Thermodyn. 7, 123-177 (1995).